



Supporting Online Material for

Deepwater Formation in the North Pacific During the Last Glacial Termination

Y. Okazaki, A. Timmermann,* L. Menviel, N. Harada, A. Abe-Ouchi, M. O. Chikamoto,
A. Mouchet, H. Asahi

*To whom correspondence should be addressed. E-mail: axel@hawaii.edu

Published 9 July 2010, *Science* **329**, 200 (2010)
DOI: 10.1126/science.1190612

This PDF file includes:

Materials and Methods

Figs. S1 to S6

Tables S1 to S5

References

Supporting Online Material for

“Deep Water Formation in the North Pacific during the Last Glacial Termination”

Y. Okazaki, A. Timmermann, L. Menviel, N. Harada, A. Abe-Ouchi, M.O. Chikamoto, A. Mouchet, H. Asahi

1. Material and Methods

Model description and experimental design

The LOVECLIM model (version 1.1) is an earth system model of intermediate complexity (EMIC) (*SI*). It consists of five coupled subsystems: a simplified 3-layer global atmosphere (ECBilt), a 3-d global ocean and thermodynamic-dynamic sea-ice model (CLIO), a simplified vegetation model (VECODE) and a global carbon cycle model (LOCH) which also includes ^{14}C and ^{13}C tracers. The physical components of the model version employed here are based on version 3 of the coupled model ECBilt-CLIO.

The global atmospheric model ECBilt is based on a quasi-geostrophic adiabatic core extended by ageostrophic corrections in T21 resolution ($\sim 5.6^\circ \times 5.6^\circ$) and three vertical layers. The daily mean irradiance used by ECBilt is calculated following Berger (*S2*).

The ocean model CLIO is a three-dimensional primitive equation model on z-coordinates with a free surface. It is coupled to a thermodynamic-dynamic sea ice model. The horizontal resolution is $3^\circ \times 3^\circ$. The globe is covered by a partly-rotated grid in the North Atlantic sector. In vertical direction, the model is divided into 20 unevenly spaced levels. Vertical mixing, mixing along isopycnals, the effect of mesoscale eddies

on transports and mixing, and downsloping currents at the bottom of continental slopes are parameterized. Bering Strait is closed in both, the pre-industrial and the Last Glacial Maximum control and freshwater perturbation simulations.

The three physical components of LOVECLIM are coupled by exchange of momentum, heat, and freshwater. The hydrological cycle is closed over land by a bucket model for soil moisture, and river runoff into the ocean.

The terrestrial vegetation module of LOVECLIM, VECODE Brovkin et al. (S3), computes once a year the evolution of the vegetation cover based on annual mean values of several climatic variables. The vegetation cover is described as a fractional distribution of desert, tree, and grass in each land grid cell.

LOCH is a 3-dimensional global model of the oceanic carbon cycle simulating dissolved inorganic carbon (DIC), total alkalinity, ^{14}C , phosphate, organic products, oxygen and silica (S4). LOCH is fully coupled to CLIO, with the same time step. In addition to their biogeochemical transformations, tracers in LOCH fully experience the circulation field predicted by CLIO. For the purpose of the simulations presented in this work the ^{14}C content at any point in the ocean is expressed as a $^{14}\text{C}/^{12}\text{C}$ ratio. Because we are focusing on timeslice experiments with fixed orbital and greenhouse gas forcing, rather than on transient deglacial runs, the production rate of ^{14}C is held constant for our experiments.

The radiocarbon tracer is only used in our pre-industrial control and freshwater perturbation simulations.

The following 2 control simulations were conducted with LOVECLIM:

1. A 10,000-year-long spin-up run was conducted using an atmospheric CO₂ concentrations of 280ppm and an atmospheric $\Delta^{14}\text{C}$ of 0 permil. The spin-up adjusts the carbon isotopes in the ocean and the global carbon cycle. The forcing is released and a fully-coupled 1500-year control run (CTR) is conducted with prognostic CO₂. Radiocarbon ages are computed from the output of this run using the computed $^{14}\text{C}/^{12}\text{C}$ ratio. In this experiment Bering Strait is closed.
2. A 3500-year-long Last Glacial Maximum Control run (LGM) using the ice-sheet topography ICE-4G of Peltier (1994), orbital forcing conditions corresponding to 21 ka B.P., greenhouse gas concentrations from 21 ka B.P. (S5). This model simulation does not include carbon isotope tracers. Bering Strait is closed in this experiment.

The following two freshwater perturbation experiments were conducted with LOVECLIM

1. A 1000-year long idealized freshwater perturbation experiment (FW-CTR) under pre-industrial conditions. By linearly increasing the freshwater forcing in the northern North Atlantic (between 50°N-70°N) for 100 years to 2 Sv, a collapse of the AMOC is triggered. Thereafter, the freshwater forcing decreases linearly for another 100 years. This experiment, although done for pre-industrial conditions (initialized from experiment CTR), mimics certain features of the climate response to Heinrich event I. In this experiment Bering Strait is closed. The carbon cycle, as well as the radiocarbon tracers are activated.
2. An LGM freshwater perturbation experiment (FW-LGM) similar to FW-CTR is conducted using glacial boundary conditions. It was initialized from experiment

LGM. For this experiment radiocarbon has not been used as a tracer. Spinning up the fully coupled carbon-cycle-climate system under LGM conditions is a major challenge that would be beyond the scope of our study. The experiment FW-LGM is used here mainly to demonstrate that also under LGM conditions the model simulates a PMOC in response to a North Atlantic freshwater pulse (Figure S2, right panel) that is very similar to the one obtained in experiment FW-CTR (Figure S2, left panel). Hence, we would expect very similar radiocarbon age anomalies in the North Pacific.

Sediment core sites information and choice of reservoir ages

Information on sediment cores sites is compiled in Table S1. The regional marine reservoir age (ΔR) is defined as the deviation of the local radiocarbon age from the globally averaged reservoir age (~ 400 yr). In the modern subarctic Pacific, ΔR ranges from ~ 200 to 500 yr (S6-10). Past marine reservoir ages may have changed significantly but are not well constrained. Therefore, we choose a constant reservoir age with a relatively large uncertainty, following a strategy proposed by Galbraith et al. (S11). For sediment cores in the subarctic Pacific and most of the eastern mid-latitude Pacific sediment cores, we choose $\Delta R = 500 \pm 300$ yr, which covers both, modern values and estimates of past ΔR (S7) in this region. This estimation enables us to evaluate calculated ventilation values in the subarctic Pacific uniformly. For core KT89-18-P4 from mid-latitude northwestern Pacific, we choose $\Delta R = 100 \pm 200$ yr based on Shishikura et al. (S12) and Yoneda et al. (S10). Note, that freshwater perturbation experiments that mimic the Heinrich event I suggest no considerable changes in surface

^{14}C ages (*S13*). Our modeling simulations conducted with LOVECLIM1.1 confirm that surface age anomalies in the North Pacific are within 200 years during a freshwater discharge experiment with an intensified Pacific Meridional Overturning Circulation (PMOC) (Figure S4). Reduction of North Atlantic surface water radiocarbon ages (Figure S4) results from an increased stratification and reduced mixing of deeper and older waters. We used $\Delta R=160\pm 150$ yr for western equatorial Pacific cores after Broecker et al. (*S14*) and $\Delta R=180\pm 300$ yr for eastern equatorial Pacific cores after Skinner and Shackleton (*S15*).

Age models

Age models for sediment cores PAR87-10, GH02-1030, MR01-K03-PC4, and BOW-9A were established based on recalculated ^{14}C dating of planktonic foraminifers (Table S2). For BOW-9A, magnetic paleointensity was used to obtain an additional age control point (21.3 ka at 305 cm (*S16*)). We converted radiocarbon ages to calendar ages with Calib 6.0 using constant reservoir age of $\Delta R=500\pm 300$ yr. We basically selected median probability of the probability distribution along the calendar year axis as age control point. Note that we have chosen age control points to minimize sedimentation rates within $\pm 1\sigma$ only in case of ^{14}C age reversals (MR01K03-PC4/5, and GH02-1003; Table S2).

Calculation for past ventilation

There are two methods of calculating paleo-ventilation ages: they can be determined

a. by calculating the ^{14}C age difference between planktonic and benthic foraminifers (BF-PF age),

b. by calculating the projection age, proposed by Adkins and Boyle (*S17*), which takes into account atmospheric $\Delta^{14}\text{C}$ changes.

Similarly, two methods to calculate paleo- ^{14}C activity for the comparison of the reconstructed benthic ^{14}C activity with the atmospheric $\Delta^{14}\text{C}$ are proposed by Galbraith et al. (*S11*):

a. simply use the contemporary atmospheric $\Delta^{14}\text{C}$ at the time of calcification, ($\Delta^{14}\text{C}_{\text{cont-atm}}$), and

b. estimate the atmospheric $\Delta^{14}\text{C}$ at the time of bottom-water formation by tracing back along the radiocarbon decay trajectory until it intersected the surface ocean $\Delta^{14}\text{C}$ record ($\Delta^{14}\text{C}_{\text{proj-atm}}$).

We used the atmospheric and surface ocean $\Delta^{14}\text{C}$ records (IntCal09 and Marine09, respectively) from Reimer et al. (*S18*). To compare these paleo- $\Delta^{14}\text{C}$ values with modern $\Delta^{14}\text{C}$ values, both $\Delta^{14}\text{C}_{\text{cont-atm}}$ and $\Delta^{14}\text{C}_{\text{proj-atm}}$ were converted to $\Delta^{14}\text{C}'_{\text{cont-atm}}$ and $\Delta^{14}\text{C}'_{\text{proj-atm}}$ as proposed by Galbraith et al. (*S11*), respectively. Definition of $\Delta^{14}\text{C}'$ is as follows:

$$\Delta^{14}\text{C}' = (\Delta^{14}\text{C}_{\text{bot}} - \Delta^{14}\text{C}_{\text{atm}}) / (\Delta^{14}\text{C}_{\text{atm}} + 1000) \times 1000\text{‰}$$

Where $\Delta^{14}\text{C}_{\text{bot}}$ is the reconstructed bottom water $\Delta^{14}\text{C}$ (calculate from ^{14}C age of benthic foraminifer (S17)), and $\Delta^{14}\text{C}_{\text{atm}}$ is the reference paleo-atmospheric $\Delta^{14}\text{C}$ (S18).

We compiled available ^{14}C ages of coexisting benthic and planktonic foraminifers in the North Pacific (Tables S3 and S5). We ruled out interpolated calendar ages in original references (S19-21) and selected new calendar ages based on planktonic foraminifera ^{14}C data except for Core MV99-GC31/PC08 (S22). Projection ages and reconstructed benthic ^{14}C activity in Core MV99-GC31/PC08 are calculated under different conditions than for the other cores. We omitted several ^{14}C records in Core VM21-30 (S21) which showed highly varied ^{14}C ages by multispecies planktonic foraminifers, suggesting substantial bioturbation impact (S14). We also omitted two ^{14}C records during the H1 interval in Core MD01-2416 (S20), which exhibit a large age reversal, suggesting bioturbation impact and/or unstable sedimentation. Planktonic foraminiferal ^{14}C ages were converted to calendar ages with Calib 6.0 using constant reservoir age as described in the previous section. We selected median probability of the probability distribution along the calendar year axis as age control point. Durations of Heinrich event 1 (H1) and Last Glacial Maximum (LGM) are 15-17.5 kyr B.P. and 19-23 kyr B.P., respectively. Reconstructed ventilation changes (^{14}C age offset between planktonic and benthic foraminifers, projection age, and intermediate-deep water $\Delta^{14}\text{C}$) in the NW Pacific and NE Pacific during 10 to 23 kyr B.P. are shown in Figs. S5 and S6, respectively. These results indicate that significant ventilation changes occurred in the NW Pacific, whereas no significant changes are found in the NE Pacific. Calculation for weighted average and uncertainty of BF–PF age, projection age, $\Delta^{14}\text{C}'_{\text{cont-atm}}$, and $\Delta^{14}\text{C}'_{\text{proj-atm}}$ follow the approach by Bevington (S23).

Stable isotope analysis of benthic foraminifer in core BOW9A

Stable isotope analyses were performed on benthic foraminifera shells (*Uvigerina* spp.) from sediment samples collected at 2.0-cm intervals in core BOW-9A. The samples were washed on a 63- μm -mesh sieve and dried in an oven at 40 °C. The dry samples were sieved through a 125- μm -mesh sieve. We then picked benthic foraminifera shells from the >125- μm fraction of each sample under a stereomicroscope. Since brownish foraminifera shells gives abnormally positive $\delta^{18}\text{O}$ and negative $\delta^{13}\text{C}$ values due to their postdepositional alterations (S24), brownish colored shells were excluded as part of our picking process. The foraminifera shells were cleaned by soaking them in 99.5% ethyl alcohol, followed by ultrasonication until all chambers were open. After confirming that all dirt had been removed, we washed the shells in 99.5% ethyl alcohol and dried them in a desiccator for 24 hours. The stable isotope measurements were performed using an IsoPrime isotope ratio mass spectrometer (GV Instruments, Manchester, United Kingdom) at the Center for Advanced Marine Core Research, Kochi University. Analyses were calibrated to the NBS-19 PDB standard, and the average analytical error to the standard was less than 0.08‰.

2. Figures

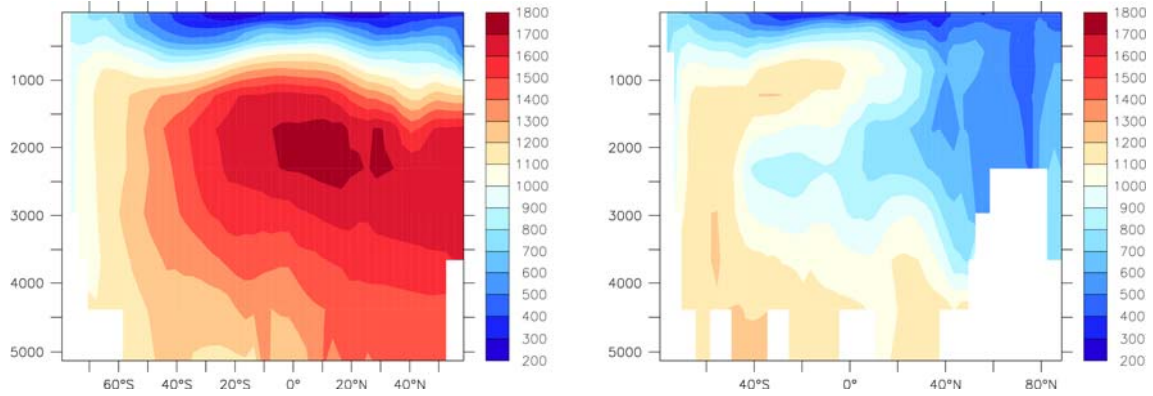


Fig. S1: Left: Pacific zonal mean section of simulated pre-bomb radiocarbon ages [years] in experiment CTR; Right: same as left, but for the Atlantic.

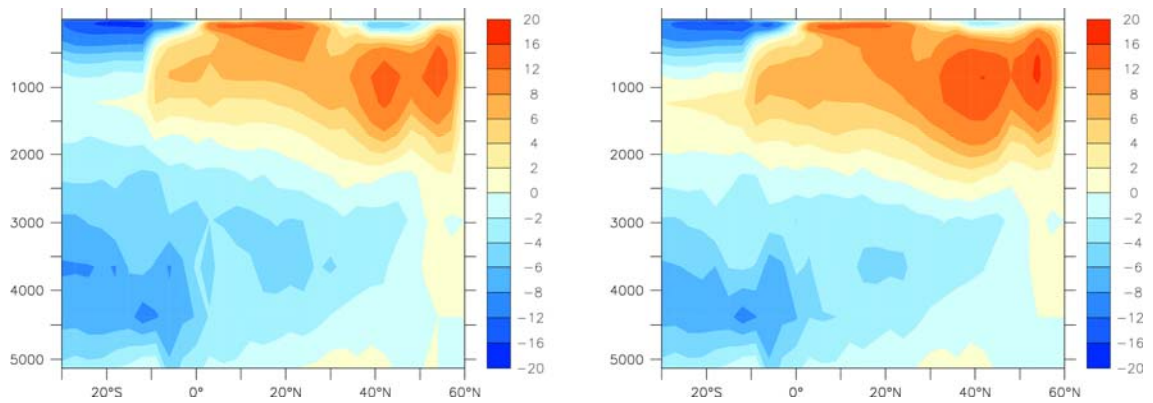


Fig. S2: Left: Pacific meridional streamfunction [$Sv=10^6 \text{ m}^3/s$] averaged over years 400-500 in experiment FW-CTR (left) and FW-LGM (right).

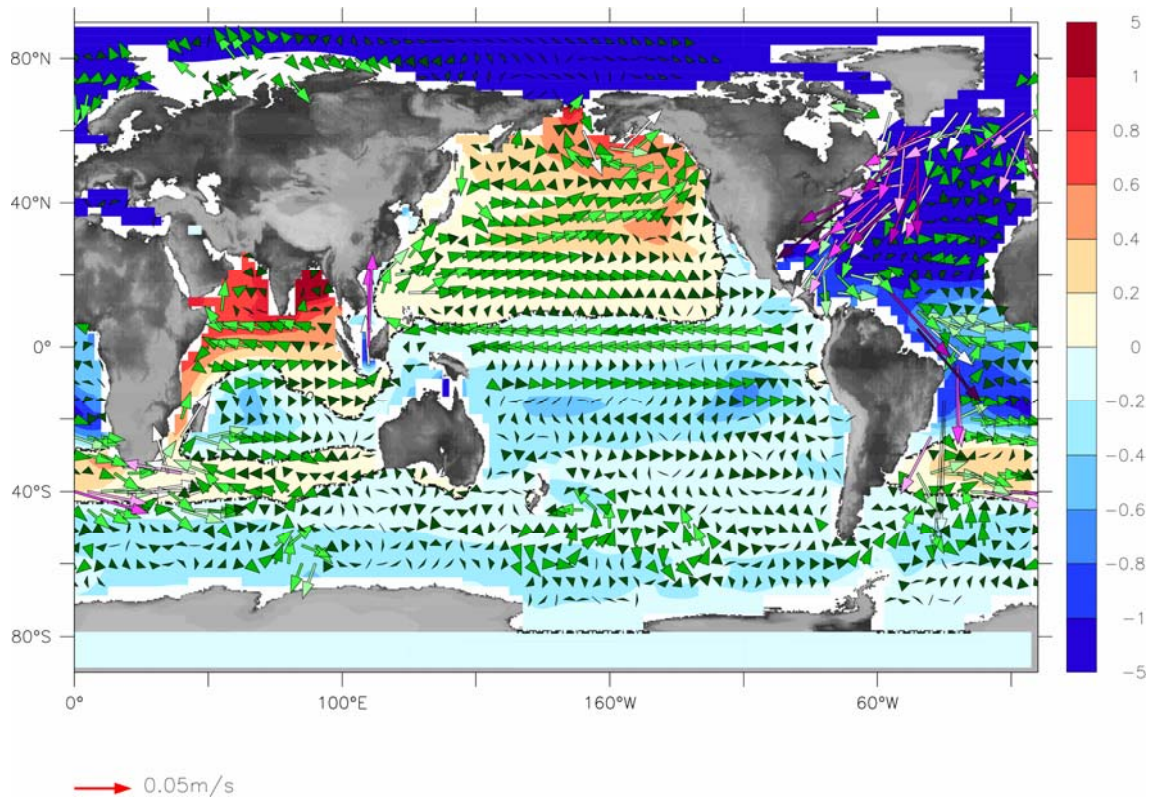


Fig. S3: Upper ocean (average over the upper 65m) currents (arrows, [cm/s]) and salinity change [psu] averaged between years 400-500 in experiment FW-CTR. Purple arrows indicate current speeds that are much larger than 0.05m/s.

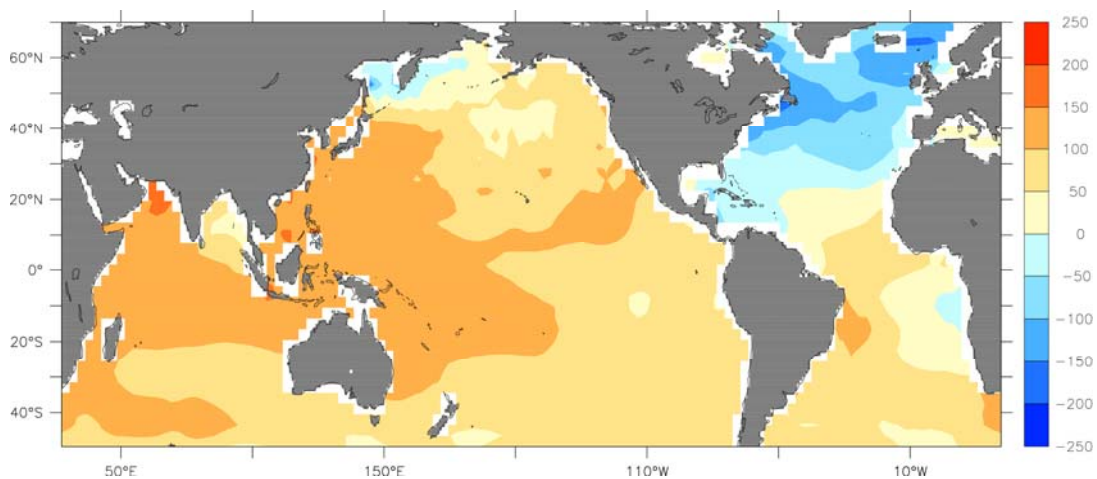


Figure S4: Upper ocean (average over the upper 50m) radiocarbon age anomalies [years] for experiment FW-CTR averaged over years 300-400.

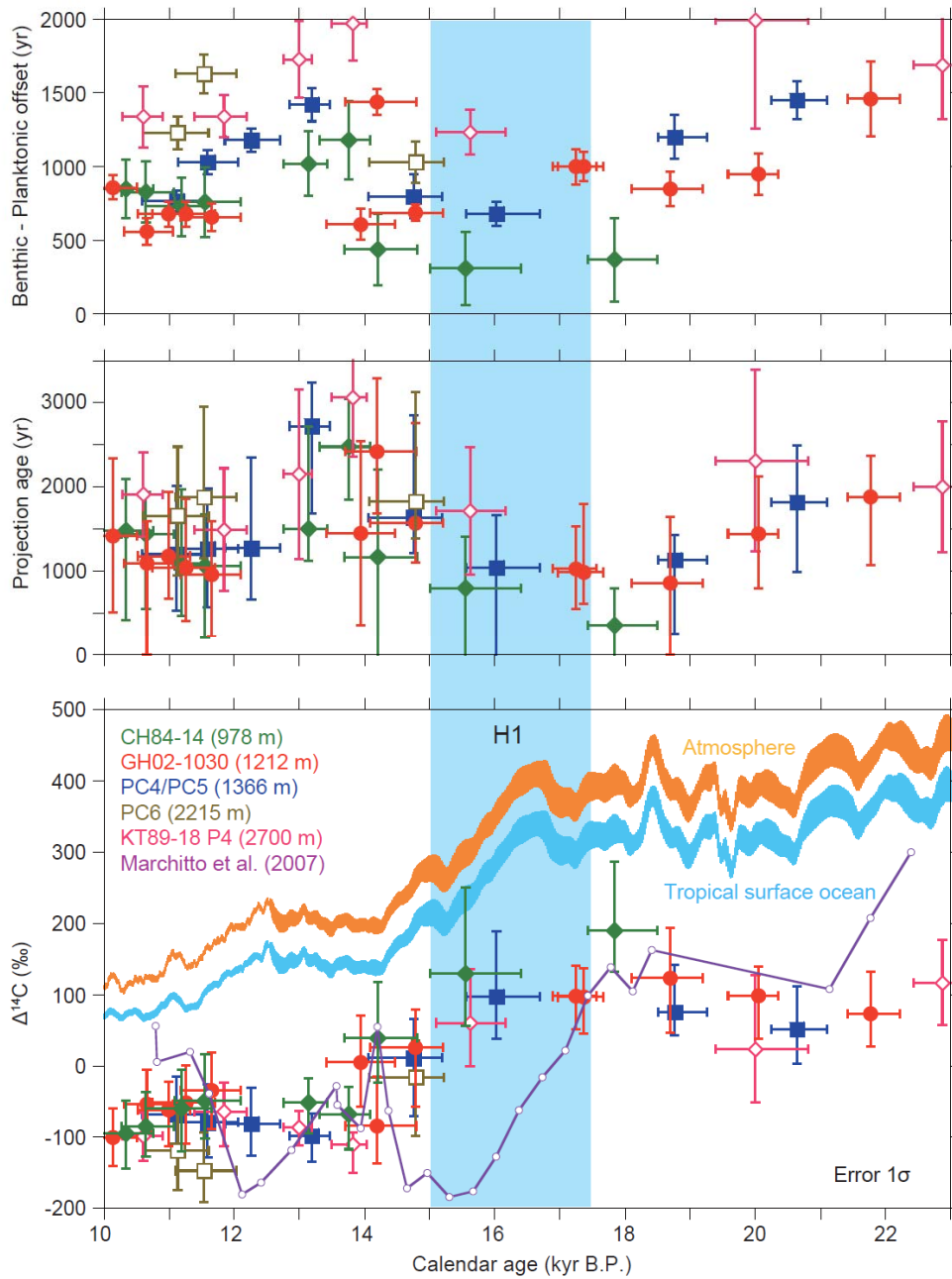


Figure S5. Ventilation changes based on BF-PF age, projection age, and $\Delta^{14}\text{C}$ in the western North Pacific ranging from 900 to 2800 m water depths. Orange and light blue curves are atmospheric (Intcal09) and surface ocean (Marine09) $\Delta^{14}\text{C}$ records (S18). Purple curve is eastern Pacific $\Delta^{14}\text{C}$ records (S22).

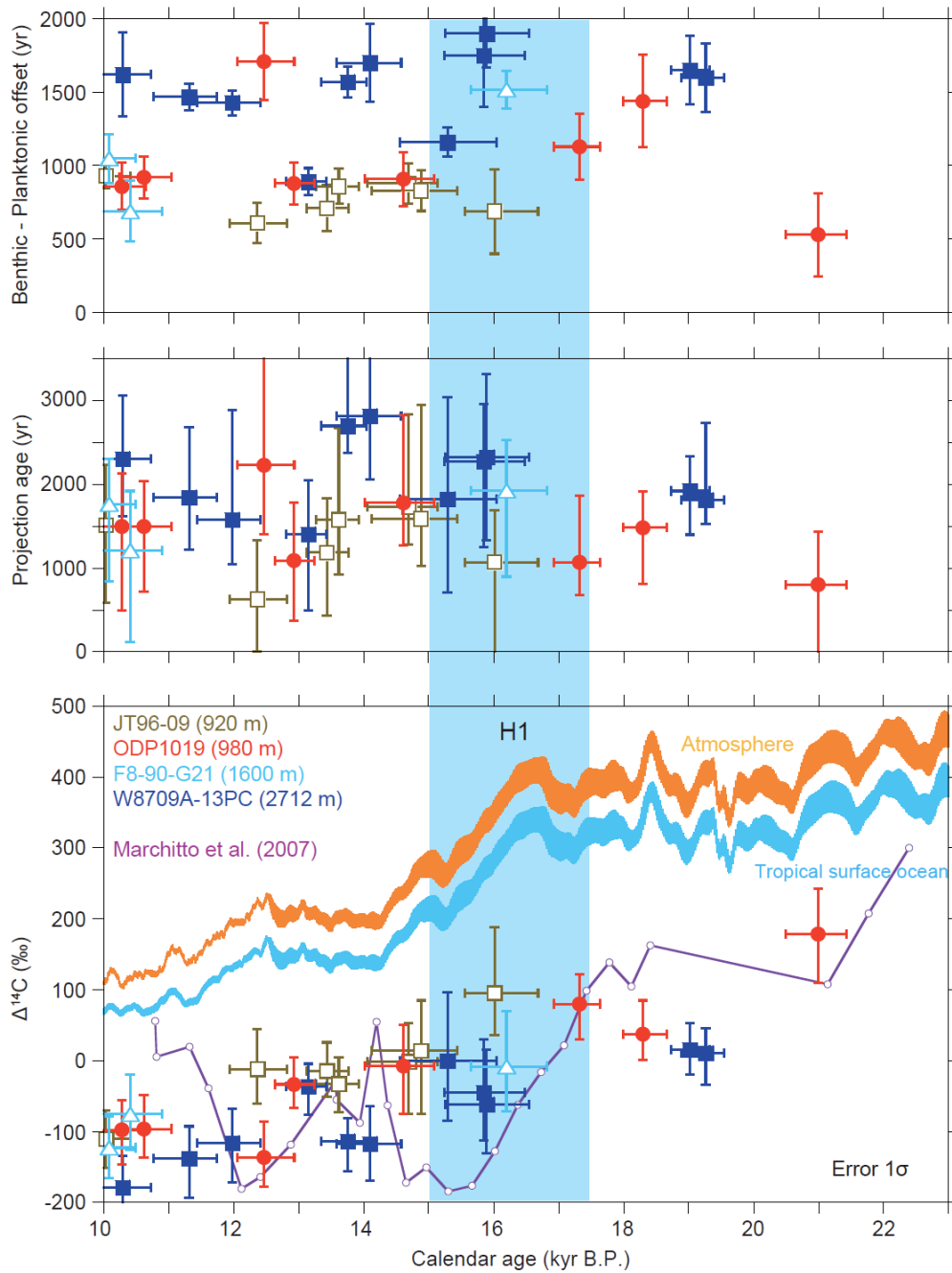


Figure S6. Ventilation changes based on BF-PF age, projection age, and $\Delta^{14}\text{C}$ in the eastern North Pacific ranging from 900 to 2800 m water depths.

3. Tables

Table S1. Sediment core lists used in this study (S11, S14, S19-22, S25-41).

| Core ID | Latitude | Longitude | Water depth (m) | Area | ΔR (yr) | Error ($\pm 1\sigma$) | Reference | Core No.* |
|----------------|----------|-----------|-----------------|-------------|-----------------|-------------------------|---|-----------|
| F2-92-P3 | 35.62°N | 121.61°W | 799 | NE Pacific | 500 | 300 | van Geen et al. (1996) | |
| F8-90-G21 | 37.22°N | 123.24°W | 1605 | NE Pacific | 500 | 300 | van Geen et al. (1996) | |
| JPC56 | 27.47°N | 112.10°W | 818 | NE Pacific | 500 | 300 | Keigwin (2002) | |
| JT96-09 | 48.91°N | 126.90°W | 920 | NE Pacific | 500 | 300 | McKay et al. (2005) | |
| ODP1019 | 41.68°N | 124.93°W | 980 | NE Pacific | 500 | 300 | Mix et al. (1999) | 7 |
| ODP887 | 54.37°N | 148.45°W | 3647 | NE Pacific | 500 | 300 | Galbraith et al. (2007) | 5 |
| ODP893 | 34.29°N | 120.04°W | 577 | NE Pacific | 500 | 300 | Kennett and Ingram (1995) | 8 |
| PAR87-10 | 54.36°N | 148.47°W | 3664 | NE Pacific | 500 | 300 | Zahn et al. (1991), de Vernal and Pedersen (1997) | |
| W8709A-13PC | 42.12°N | 125.75°W | 2712 | NE Pacific | 500 | 300 | Mix et al. (1999) | 6 |
| CH84-14 | 41.73°N | 142.55°E | 978 | NW Pacific | 500 | 300 | Duplessy et al. (1989) | |
| GH02-1030 | 42.23°N | 144.21°E | 1212 | NW Pacific | 500 | 300 | Ikehara et al. (2006), Sagawa and Ikehara (2008) | 1 |
| KR02-15-PC6 | 40.40°N | 143.50°E | 2215 | NW Pacific | 500 | 300 | Minoshima et al. (2007) | |
| KT89-18-P4 | 32.15°N | 133.90°E | 2700 | NW Pacific | 100 | 200 | Murayama et al. (1992) | 3 |
| MD01-2416 | 51.27°N | 167.73°E | 2317 | NW Pacific | 500 | 300 | Sarnthein et al. (2006) | |
| MR01K03-PC4/5 | 41.12°N | 142.40°E | 1366 | NW Pacific | 500 | 300 | Ahagon et al. (2003), Hoshiba et al. (2006) | 2 |
| ODP883 | 51.20°N | 167.77°E | 2385 | NW Pacific | 500 | 300 | Sarnthein et al. (2006) | |
| BOW9A | 54.04°N | 178.68°E | 2391 | Bering Sea | 500 | 300 | Okazaki et al. (2005) | |
| B34-91 | 49.0°N | 150.3°E | 1227 | Okhotsk Sea | 500 | 300 | Keigwin (2002) | |
| GGC15 | 48.6°N | 150.4°E | 1980 | Okhotsk Sea | 500 | 300 | Keigwin (2002) | |
| GGC18 | 48.8°N | 150.4°E | 1700 | Okhotsk Sea | 500 | 300 | Keigwin (2002) | |
| GGC20 | 48.9°N | 150.4°E | 1510 | Okhotsk Sea | 500 | 300 | Keigwin (2002) | |
| GGC27 | 49.6°N | 150.2°E | 995 | Okhotsk Sea | 500 | 300 | Keigwin (2002) | |
| MV99-GC31/PC08 | 23.5°N | 111.6°W | 705 | E Pacific | 200 | 100 | Marchitto et al. (2007) | 9 |
| TR163-31 | 3.62°S | 83.97°W | 3210 | E Pacific | 150 | 300 | Shackleton et al. (1988) | |
| VM21-30 | 1.22°S | 89.68°W | 617 | E Pacific | 150 | 300 | Stott et al. (2009) | 10 |
| 50-37KL | 18.9°N | 115.77°E | 2695 | W Pacific | 160 | 150 | Broecker et al. (1990) | |
| MD01-2386 | 1°N | 130°E | 2800 | W Pacific | 160 | 150 | Broecker et al. (2008) | 4 |
| MD97-2138 | 1°S | 146°E | 1900 | W Pacific | 160 | 150 | Broecker et al. (2004) | |
| MD98-2181 | 6°N | 126°E | 2100 | W Pacific | 160 | 150 | Broecker et al. (2004) | |

*Numbers are as same as the numbers in symbols in Figures 3.

Table S2. Age control points for cores PAR87A-10, MR01K03-PC4/5, GH02-1030, and BOW9A (S37, S33, S38).

Selected ages are the probability median values except for ages with asterisk which were determined to minimize sedimentation rates.

| Core ID | Depth (cm) | Planktonic ¹⁴ C age (yr B.P.) | Error ±1σ (yr) | Probability median ±1σ (yr B.P.) | Calendar age (yr B.P.) | +1σ | -1σ | Selected age (yr B.P.) | Species | Lab Code** | Original reference |
|---------------|------------|--|----------------|----------------------------------|------------------------|-------|--------|------------------------|----------------------|------------|-----------------------|
| PAR87A-10 | 23 | 6640 | 300 | 6589 | 6166 | 7099 | 6589 | 6589 | <i>N. pachyderma</i> | RIDDL | Zahn et al. (1991) |
| PAR87A-10 | 50 | 12490 | 230 | 13476 | 13083 | 13881 | 13476 | 13476 | <i>G. bulloides</i> | RIDDL | Zahn et al. (1991) |
| PAR87A-10 | 121 | 16670 | 560 | 18963 | 18088 | 19570 | 18963 | 18963 | <i>N. pachyderma</i> | RIDDL | Zahn et al. (1991) |
| PAR87A-10 | 213 | 31600 | | 34699 | 32232 | 36634 | 34699 | 34699 | <i>N. pachyderma</i> | RIDDL | Zahn et al. (1991) |
| MR01K03-PC4/5 | 16.9 | 3290 | 40 | 2515 | 2125 | 2866 | 2515 | 2515 | <i>N. pachyderma</i> | IAA | Hoshiba et al. (2006) |
| MR01K03-PC4/5 | 39.6 | 4270 | 100 | 3735 | 3332 | 4141 | 3735 | 3735 | <i>N. pachyderma</i> | IAA | Hoshiba et al. (2006) |
| MR01K03-PC4/5 | 62.8 | 5450 | 110 | 5236 | 4842 | 5601 | 5236 | 5236 | <i>N. pachyderma</i> | IAA | Hoshiba et al. (2006) |
| MR01K03-PC4/5 | 100.7 | 7500 | 110 | 7487 | 7184 | 7816 | 7487 | 7487 | <i>N. pachyderma</i> | IAA | Hoshiba et al. (2006) |
| MR01K03-PC4/5 | 144.4 | 8720 | 50 | 8775 | 8392 | 9115 | 8775 | 8775 | <i>N. pachyderma</i> | IAA | Hoshiba et al. (2006) |
| MR01K03-PC4/5 | 185 | 9280 | 40 | 9458 | 9060 | 9858 | 9458 | 9458 | <i>N. pachyderma</i> | NIES-TERRA | Hoshiba et al. (2006) |
| MR01K03-PC4/5 | 230.2 | 10600 | 50 | 11115 | 10588 | 11414 | 11115 | 11115 | <i>N. pachyderma</i> | IAA | Hoshiba et al. (2006) |
| MR01K03-PC4/5 | 262.1 | 10900 | 60 | 11589 | 11134 | 12060 | 11589 | 11589 | Mixed planktonic | NOSAMS | Hoshiba et al. (2006) |
| MR01K03-PC4/5 | 292.5 | 11420 | 60 | 12263 | 11857 | 12705 | 12263 | 12263 | <i>N. pachyderma</i> | IAA | Hoshiba et al. (2006) |
| MR01K03-PC4/5 | 313.2 | 12230 | 50 | 13191 | 12846 | 13470 | 13191 | 13191 | <i>N. pachyderma</i> | IAA | Hoshiba et al. (2006) |
| MR01K03-PC4/5 | 335.8 | 12400 | 50 | 13367 | 13099 | 13715 | 13367 | 13367 | <i>N. pachyderma</i> | NOSAMS | Hoshiba et al. (2006) |
| MR01K03-PC4/5 | 363.3 | 13450 | 90 | 14757 | 14059 | 15188 | 14757 | 14757 | Mixed planktonic | NOSAMS | Hoshiba et al. (2006) |
| MR01K03-PC4/5 | 405.5 | 14150 | 60 | 16028 | 15567 | 16692 | 15780* | 15780* | Mixed planktonic | NOSAMS | Hoshiba et al. (2006) |
| MR01K03-PC4/5 | 413 | 13690 | 60 | 15263 | 14534 | 15957 | 15957* | 15957* | <i>N. pachyderma</i> | IAA | Hoshiba et al. (2006) |
| MR01K03-PC4/5 | 540 | 16450 | 110 | 18763 | 18513 | 19262 | 18763 | 18763 | Mixed planktonic | NOSAMS | Hoshiba et al. (2006) |
| MR01K03-PC4/5 | 642 | 18200 | 70 | 20638 | 20244 | 21102 | 20638 | 20638 | Mixed planktonic | NOSAMS | Hoshiba et al. (2006) |
| MR01K03-PC4/5 | 844.7 | 21500 | 110 | 24587 | 24219 | 24996 | 24587 | 24587 | Mixed planktonic | NOSAMS | Hoshiba et al. (2006) |
| MR01K03-PC4/5 | 945.6 | 23560 | 110 | 27316 | 26901 | 27810 | 27316 | 27316 | Mixed planktonic | IAA | Hoshiba et al. (2006) |
| MR01K03-PC4/5 | 1082.3 | 25700 | 150 | 29677 | 29398 | 30166 | 29677 | 29677 | Mixed planktonic | NOSAMS | Hoshiba et al. (2006) |
| MR01K03-PC4/5 | 1322 | 30130 | 180 | 33874 | 33500 | 34454 | 33874 | 33874 | Mixed planktonic | IAA | Hoshiba et al. (2006) |

**AA, NSF-Arizona AMS Laboratory, University of Arizona; OS, National Ocean Sciences AMS facility, Woods Hole Oceanographic Institution

RIDDL, Radio-Isotope Direct Detection Laboratory at Simon Fraser University; IAA, Institute of Accelerator Analysis Ltd., Shirakawa, Japan

NIES-TERRA: National Institute for Environmental Studies, Tsukuba, Japan.; Beta, Beta Analytic Inc.

Table S2. (cont.)

Selected ages are the probability median values except for ages with asterisk which were determined to minimize sedimentation rates.

| Core ID | Depth (cm) | Planktonic ¹⁴ C age (yr B.P.) | Error $\pm 1\sigma$ (yr) | Probability median (yr B.P.) | Calendar age (yr B.P.) | -1 σ | +1 σ | Selected age (yr B.P.) | Species | Lab Code** | Original reference |
|-----------|------------|--|--------------------------|------------------------------|------------------------|-------------|-------------|------------------------|----------------------|------------|-----------------------|
| GH02-1030 | 210 | 9840 | 40 | 10134 | 10134 | 9751 | 10506 | 10134 | Mixed planktonic | Beta188642 | Ikehara et al. (2006) |
| GH02-1030 | 220 | 10240 | 60 | 10656 | 10656 | 10310 | 11065 | 10656 | Mixed planktonic | Beta175956 | Ikehara et al. (2006) |
| GH02-1030 | 235 | 10510 | 60 | 10986 | 10986 | 10524 | 11329 | 10986 | Mixed planktonic | Beta175958 | Ikehara et al. (2006) |
| GH02-1030 | 244 | 10690 | 60 | 11261 | 11261 | 10743 | 11703 | 11261 | Mixed planktonic | Beta175960 | Ikehara et al. (2006) |
| GH02-1030 | 261 | 10950 | 60 | 11654 | 11654 | 11181 | 12100 | 11654 | <i>N. pachyderma</i> | Beta175962 | Ikehara et al. (2006) |
| GH02-1030 | 290 | 12900 | 70 | 13943 | 13943 | 13412 | 14241 | 13943 | <i>N. pachyderma</i> | Beta175964 | Ikehara et al. (2006) |
| GH02-1030 | 307.5 | 13270 | 70 | 14498 | 14498* | 13981 | 14970 | 14208* | <i>N. pachyderma</i> | Beta175966 | Ikehara et al. (2006) |
| GH02-1030 | 323.5 | 13060 | 70 | 14193 | 14193 | 13702 | 14647 | 14450* | Mixed planktonic | Beta175968 | Ikehara et al. (2006) |
| GH02-1030 | 345.5 | 13470 | 40 | 14783 | 14783 | 14082 | 15204 | 14783 | <i>N. pachyderma</i> | Beta175970 | Ikehara et al. (2006) |
| GH02-1030 | 403.5 | 15090 | 50 | 17323 | 17323 | 16946 | 17619 | 16946* | Mixed planktonic | Beta175973 | Ikehara et al. (2006) |
| GH02-1030 | 435.5 | 15010 | 80 | 17245 | 17245 | 16889 | 17560 | 17318* | Mixed planktonic | Beta175975 | Ikehara et al. (2006) |
| GH02-1030 | 465.5 | 15140 | 60 | 17369 | 17369 | 16976 | 17666 | 17666* | Mixed planktonic | Beta188643 | Ikehara et al. (2006) |
| GH02-1030 | 523 | 16380 | 60 | 18692 | 18692 | 18477 | 18961 | 18692 | Mixed planktonic | Beta175979 | Ikehara et al. (2006) |
| GH02-1030 | 558 | 17780 | 70 | 20051 | 20051 | 19772 | 20352 | 20051 | Mixed planktonic | Beta175981 | Ikehara et al. (2006) |
| GH02-1030 | 630 | 19130 | 180 | 21770 | 21770 | 21413 | 22214 | 21770 | Mixed planktonic | Beta175429 | Ikehara et al. (2006) |
| BOW9A | 49 | 4025 | 41 | 3419 | 3419 | 3037 | 3805 | 3419 | <i>N. pachyderma</i> | AA68045 | This study |
| BOW9A | 73 | 5662 | 46 | 5494 | 5494 | 5177 | 5883 | 5494 | <i>N. pachyderma</i> | AA68046 | This study |
| BOW9A | 104 | 8480 | 260 | 8516 | 8516 | 8055 | 8965 | 8516 | <i>N. pachyderma</i> | AA68044 | This study |
| BOW9A | 136 | 10519 | 91 | 11001 | 11001 | 10517 | 11359 | 11001 | <i>N. pachyderma</i> | AA68040 | This study |
| BOW9A | 140 | 10850 | 60 | 11521 | 11521 | 11087 | 12031 | 11521 | <i>N. pachyderma</i> | OS57380 | This study |
| BOW9A | 168 | 12850 | 50 | 13869 | 13869 | 13389 | 14181 | 13869 | <i>N. pachyderma</i> | OS57381 | This study |
| BOW9A | 176 | 13018 | 69 | 14124 | 14124 | 13616 | 14593 | 14124 | <i>N. pachyderma</i> | AA68041 | This study |
| BOW9A | 192 | 13209 | 74 | 14420 | 14420 | 13910 | 14895 | 14420 | <i>N. pachyderma</i> | AA68042 | This study |

**AA, NSF-Arizona AMS Laboratory, University of Arizona; OS, National Ocean Sciences AMS facility, Woods Hole Oceanographic Institution
 RIDD, Radio-Isotope Direct Detection Laboratory at Simon Fraser University; IAA, Institute of Accelerator Analysis Ltd., Shirakawa, Japan
 NIES-TERRA: National Institute for Environmental Studies, Tsukuba, Japan.; Beta, Beta Analytic Inc.

Table S3. cont.

Durations of BA, H1, and LGM are 13-14.5 ka, 15-17.5 ka, and 19-23 ka, respectively.

| Core ID | Water depth (m) | Core depth (cm) | Calendar age (yr) | -1 σ (yr) | +1 σ (yr) | PF ¹⁴ C (yr) | \pm 1 σ (yr) | BF ¹⁴ C (yr) | \pm 1 σ (yr) | BF-PF (yr) | \pm 1 σ (yr) | Projection (yr) | -1 σ (yr) | +1 σ (yr) | Era |
|-------------|--------------------|--------------------|----------------------|---------------------|---------------------|----------------------------|--------------------------|----------------------------|--------------------------|---------------|--------------------------|--------------------|---------------------|---------------------|-----|
| PC08 | 705 | 456.5 | 14960 | 200 | 200 | N/A | N/A | 15850 | 40 | N/A | N/A | 3490 | 214 | 294 | |
| PC08 | 705 | 466 | 15300 | 300 | 300 | N/A | N/A | 16505 | 40 | N/A | N/A | 3900 | 651 | 201 | H1 |
| PC08 | 705 | 476.5 | 15670 | 300 | 300 | N/A | N/A | 16785 | 45 | N/A | N/A | 3580 | 285 | 385 | H1 |
| PC08 | 705 | 486.5 | 16020 | 300 | 300 | N/A | N/A | 16665 | 40 | N/A | N/A | 3210 | 594 | 284 | H1 |
| PC08 | 705 | 496.5 | 16370 | 300 | 300 | N/A | N/A | 16425 | 45 | N/A | N/A | 2730 | 587 | 277 | H1 |
| PC08 | 705 | 506.5 | 16730 | 300 | 300 | N/A | N/A | 16390 | 40 | N/A | N/A | 2100 | 327 | 537 | H1 |
| PC08 | 705 | 516.5 | 17080 | 300 | 300 | N/A | N/A | 16425 | 50 | N/A | N/A | 2020 | 579 | 279 | H1 |
| PC08 | 705 | 526.5 | 17430 | 300 | 300 | N/A | N/A | 16185 | 45 | N/A | N/A | 1250 | 332 | 612 | H1 |
| PC08 | 705 | 536.5 | 17780 | 300 | 300 | N/A | N/A | 16235 | 40 | N/A | N/A | 920 | 322 | 622 | |
| PC08 | 705 | 547 | 18120 | 300 | 300 | N/A | N/A | 16810 | 40 | N/A | N/A | 1140 | 221 | 561 | |
| PC08 | 705 | 556 | 18410 | 300 | 300 | N/A | N/A | 16680 | 40 | N/A | N/A | 820 | 569 | 289 | |
| PC08 | 705 | 641.5 | 21140 | 200 | 200 | N/A | N/A | 19720 | 60 | N/A | N/A | 1680 | 462 | 412 | LGM |
| PC08 | 705 | 661.5 | 21770 | 300 | 300 | N/A | N/A | 19640 | 60 | N/A | N/A | 990 | 589 | 519 | LGM |
| PC08 | 705 | 680.8 | 22390 | 300 | 300 | N/A | N/A | 19650 | 80 | N/A | N/A | 370 | 579 | 529 | LGM |
| PC4/PC5 | 1366 | 231-232 | 11115 | 527 | 462 | 10600 | 50 | 11370 | 50 | 770 | 71 | 1205 | 667 | 812 | |
| PC4/PC5 | 1366 | 262-264 | 11589 | 454 | 469 | 10900 | 55 | 11930 | 60 | 1030 | 81 | 1271 | 692 | 717 | |
| PC4/PC5 | 1366 | 291-293 | 12263 | 406 | 442 | 11420 | 60 | 12600 | 50 | 1180 | 78 | 1277 | 607 | 1081 | |
| PC4/PC5 | 1366 | 311-313 | 13191 | 345 | 279 | 12230 | 50 | 13650 | 100 | 1420 | 112 | 2729 | 1039 | 515 | BA |
| PC4/PC5 | 1366 | 363-365 | 14756 | 694 | 430 | 13450 | 85 | 14250 | 120 | 800 | 147 | 1644 | 424 | 1208 | |
| PC4/PC5 | 1366 | 405-407 | 16029 | 461 | 662 | 14150 | 55 | 14830 | 60 | 680 | 81 | 1051 | 1093 | 622 | H1 |
| PC4/PC5 | 1366 | 540-542 | 18763 | 250 | 499 | 16450 | 110 | 17650 | 100 | 1200 | 149 | 1137 | 873 | 304 | |
| PC4/PC5 | 1366 | 642-644 | 20638 | 393 | 462 | 18200 | 65 | 19650 | 110 | 1450 | 128 | 1822 | 826 | 677 | LGM |
| TR163-31 | 3210 | 83-87 | 17291 | 429 | 381 | 14728 | 222 | 15660 | 270 | 932 | 349 | 1099 | 761 | 519 | H1 |
| TR163-31 | 3210 | 114 | 19269 | 446 | 492 | 16700 | 260 | 19510 | 330 | 2810 | 420 | 3151 | 574 | 998 | LGM |
| VM21-30 | 617 | 139 | 10848 | 369 | 351 | 10079 | 26 | 15350 | 360 | 5271 | 361 | 7032 | 471 | 749 | |
| VM21-30 | 617 | 143 | 10587 | 369 | 461 | 9867 | 145 | 16550 | 390 | 6683 | 416 | 8643 | 882 | 370 | |
| VM21-30 | 617 | 177 | 13233 | 334 | 335 | 11952 | 25 | 20027 | 406 | 8075 | 407 | 10047 | 647 | 576 | BA |
| VM21-30 | 617 | 182 | 13594 | 486 | 423 | 12265 | 272 | 18650 | 380 | 6385 | 468 | 7846 | 471 | 994 | BA |
| VM21-30 | 617 | 201-202 | 16506 | 864 | 683 | 14216 | 356 | 20320 | 80 | 6104 | 365 | 7134 | 1068 | 1409 | H1 |
| VM21-30 | 617 | 236 | 20087 | 506 | 303 | 17490 | 85 | 19120 | 110 | 1630 | 139 | 2063 | 368 | 931 | LGM |
| VM21-30 | 617 | 241 | 19546 | 586 | 417 | 16950 | 302 | 21505 | 137 | 4554 | 332 | 5354 | 645 | 1194 | LGM |
| W8709A-13PC | 2712 | 126.25 | 10291 | 553 | 432 | 9960 | 230 | 11580 | 170 | 1620 | 286 | 2309 | 687 | 758 | |
| W8709A-13PC | 2712 | 139 | 11313 | 549 | 430 | 10720 | 70 | 12190 | 60 | 1470 | 92 | 1847 | 620 | 839 | |
| W8709A-13PC | 2712 | 154 | 11979 | 543 | 436 | 11200 | 60 | 12630 | 60 | 1430 | 85 | 1581 | 527 | 1314 | |
| W8709A-13PC | 2712 | 170.5 | 13151 | 343 | 272 | 12190 | 60 | 13080 | 70 | 890 | 92 | 1409 | 914 | 645 | BA |
| W8709A-13PC | 2712 | 191.5 | 13752 | 409 | 294 | 12760 | 60 | 14330 | 90 | 1570 | 108 | 2698 | 320 | 815 | BA |
| W8709A-13PC | 2712 | 198.75 | 14099 | 508 | 477 | 13000 | 90 | 14700 | 250 | 1700 | 266 | 2821 | 755 | 826 | BA |
| W8709A-13PC | 2712 | 212.5 | 15289 | 730 | 760 | 13700 | 70 | 14860 | 70 | 1160 | 99 | 1831 | 1116 | 1216 | H1 |
| W8709A-13PC | 2712 | 221.25 | 15889 | 633 | 650 | 14050 | 140 | 15950 | 180 | 1900 | 228 | 2331 | 989 | 982 | H1 |
| W8709A-13PC | 2712 | 223.75 | 15849 | 607 | 621 | 14020 | 140 | 15770 | 320 | 1750 | 349 | 2271 | 1012 | 688 | H1 |
| W8709A-13PC | 2712 | 301.25 | 19018 | 291 | 304 | 16710 | 120 | 18360 | 200 | 1650 | 233 | 1922 | 517 | 414 | LGM |
| W8709A-13PC | 2712 | 303.75 | 19261 | 376 | 282 | 17030 | 150 | 18630 | 180 | 1600 | 234 | 1819 | 290 | 914 | LGM |

Table S4. Reconstructed ventilation ages and bottom-water $\Delta^{14}\text{C}$ values in the North Pacific sediments.

Durations of BA, H1, and LGM are 13-14.5 ka, 15-17.5 ka, and 19-23 ka, respectively.

| Core ID | Water depth (m) | Core depth (cm) | Calendar age (yr) | -1 σ (yr) | +1 σ (yr) | Bottom $\Delta^{14}\text{C}$ (‰) | -1 σ (yr) | +1 σ (yr) | $\Delta^{14}\text{C}'$ cont-atm (‰) | -1 σ (yr) | +1 σ (yr) | $\Delta^{14}\text{C}'$ proj-atm (‰) | -1 σ (yr) | +1 σ (yr) | Era |
|-------------|--------------------|--------------------|----------------------|---------------------|---------------------|-------------------------------------|---------------------|---------------------|--|---------------------|---------------------|--|---------------------|---------------------|-----|
| 50-37KL | 2695 | 160-165 | 17832 | 282 | 587 | 29 | 35 | 76 | -266 | 57 | 91 | -234 | 79 | 68 | |
| 50-37KL | 2695 | 175-180 | 18582 | 403 | 208 | 81 | 51 | 28 | -234 | 78 | 59 | -223 | 55 | 44 | |
| 50-37KL | 2695 | 195-200 | 19946 | 351 | 252 | 57 | 44 | 33 | -235 | 62 | 54 | -276 | 49 | 50 | LGM |
| 50-37KL | 2695 | 205-210 | 20043 | 426 | 256 | 4 | 50 | 32 | -279 | 60 | 56 | -297 | 96 | 56 | LGM |
| CH84-14 | 978 | 230 | 10341 | 465 | 411 | -95 | 50 | 46 | -185 | 62 | 51 | -257 | 62 | 90 | |
| CH84-14 | 978 | 280 | 10644 | 383 | 432 | -85 | 41 | 49 | -188 | 57 | 64 | -249 | 49 | 67 | |
| CH84-14 | 978 | 310 | 11190 | 547 | 461 | -60 | 60 | 54 | -185 | 68 | 79 | -217 | 75 | 57 | |
| CH84-14 | 978 | 340 | 11550 | 467 | 551 | -49 | 52 | 66 | -181 | 78 | 83 | -214 | 57 | 74 | |
| CH84-14 | 978 | 400 | 13142 | 386 | 289 | -52 | 43 | 34 | -215 | 48 | 41 | -254 | 105 | 64 | BA |
| CH84-14 | 978 | 480 | 13756 | 454 | 336 | -68 | 50 | 39 | -225 | 50 | 46 | -337 | 57 | 58 | BA |
| CH84-14 | 978 | 510 | 14207 | 511 | 604 | 39 | 62 | 79 | -131 | 102 | 88 | -223 | 131 | 152 | BA |
| CH84-14 | 978 | 550 | 15554 | 550 | 844 | 129 | 73 | 121 | -131 | 144 | 153 | -186 | 113 | 184 | H1 |
| CH84-14 | 978 | 690 | 17839 | 409 | 651 | 190 | 57 | 97 | -151 | 86 | 115 | -143 | 100 | 114 | |
| F2-92-P3 | 800 | 120 | 10367 | 456 | 385 | -184 | 44 | 39 | -269 | 53 | 47 | -324 | 49 | 49 | |
| F2-92-P3 | 800 | 140 | 11151 | 542 | 467 | -91 | 58 | 53 | -213 | 63 | 80 | -250 | 60 | 65 | |
| F2-92-P3 | 800 | 163 | 12783 | 378 | 391 | -21 | 44 | 47 | -184 | 62 | 49 | -182 | 92 | 65 | |
| F2-92-P3 | 800 | 160 | 13112 | 362 | 285 | -34 | 41 | 34 | -203 | 43 | 44 | -244 | 56 | 93 | BA |
| F2-92-P3 | 800 | 170 | 14330 | 520 | 516 | 26 | 63 | 66 | -150 | 98 | 86 | -269 | 100 | 164 | BA |
| F2-92-P3 | 800 | 200 | 18959 | 307 | 371 | 109 | 40 | 51 | -185 | 72 | 53 | -197 | 55 | 58 | |
| F2-92-P3 | 800 | 214 | 12733 | 380 | 488 | -25 | 44 | 59 | -188 | 63 | 60 | -186 | 89 | 76 | |
| F2-92-P3 | 800 | 298 | 14072 | 569 | 459 | -1 | 66 | 57 | -164 | 83 | 64 | -287 | 105 | 153 | BA |
| F8-90-G21 | 1600 | 75 | 10084 | 412 | 401 | -123 | 43 | 44 | -219 | 45 | 67 | -282 | 52 | 79 | |
| F8-90-G21 | 1600 | 83 | 10406 | 460 | 485 | -75 | 50 | 56 | -172 | 59 | 62 | -226 | 80 | 97 | |
| F8-90-G21 | 1600 | 155 | 16192 | 540 | 627 | -8 | 63 | 78 | -279 | 104 | 119 | -292 | 93 | 104 | H1 |
| B34-91 | 1227 | 225 | 19449 | 490 | 383 | 32 | 59 | 49 | -251 | 83 | 72 | -267 | 97 | 56 | LGM |
| GGC15 | 1980 | 170 | 19920 | 362 | 305 | 20 | 44 | 38 | -261 | 63 | 58 | -294 | 57 | 55 | LGM |
| GGC18 | 1700 | 214-216 | 18547 | 487 | 314 | 28 | 59 | 40 | -278 | 76 | 81 | -251 | 114 | 58 | |
| GGC20 | 1510 | 230 | 19635 | 295 | 451 | 49 | 37 | 59 | -219 | 81 | 56 | -268 | 66 | 76 | LGM |
| GGC27 | 995 | 70 | 19050 | 295 | 343 | 40 | 36 | 44 | -240 | 68 | 52 | -278 | 59 | 84 | LGM |
| GH02-1030 | 1212 | 210 | 10134 | 383 | 372 | -101 | 41 | 41 | -201 | 41 | 63 | -248 | 71 | 79 | |
| GH02-1030 | 1212 | 220 | 10656 | 346 | 409 | -54 | 39 | 48 | -159 | 55 | 60 | -216 | 61 | 92 | |
| GH02-1030 | 1212 | 235 | 10986 | 462 | 343 | -62 | 51 | 40 | -185 | 56 | 67 | -221 | 66 | 45 | |
| GH02-1030 | 1212 | 244 | 11261 | 518 | 442 | -52 | 58 | 52 | -168 | 78 | 64 | -211 | 72 | 56 | |
| GH02-1030 | 1212 | 261 | 11654 | 473 | 446 | -35 | 54 | 54 | -172 | 78 | 76 | -202 | 57 | 63 | |
| GH02-1030 | 1212 | 290 | 13943 | 531 | 518 | 5 | 63 | 65 | -161 | 73 | 71 | -249 | 134 | 137 | BA |
| GH02-1030 | 1212 | 323.5 | 14193 | 491 | 598 | -84 | 53 | 69 | -234 | 90 | 80 | -332 | 74 | 74 | BA |
| GH02-1030 | 1212 | 345.5 | 14783 | 701 | 421 | 26 | 83 | 54 | -187 | 100 | 107 | -260 | 96 | 75 | |
| GH02-1030 | 1212 | 435.5 | 17245 | 356 | 315 | 98 | 46 | 43 | -195 | 65 | 46 | -210 | 59 | 60 | H1 |
| GH02-1030 | 1212 | 465.5 | 17369 | 393 | 297 | 96 | 51 | 40 | -207 | 60 | 56 | -205 | 72 | 55 | H1 |
| GH02-1030 | 1212 | 523 | 18692 | 587 | 503 | 123 | 77 | 70 | -191 | 111 | 97 | -194 | 82 | 95 | |
| GH02-1030 | 1212 | 558 | 20051 | 471 | 301 | 99 | 61 | 41 | -212 | 69 | 68 | -249 | 70 | 78 | LGM |
| GH02-1030 | 1212 | 630 | 21770 | 357 | 444 | 73 | 45 | 59 | -249 | 76 | 76 | -287 | 52 | 69 | LGM |
| JPC56 | 818 | 649-651 | 10504 | 350 | 491 | -42 | 40 | 59 | -146 | 51 | 68 | -186 | 70 | 90 | |
| JPC56 | 818 | 899-901 | 11648 | 474 | 453 | -4 | 56 | 56 | -146 | 80 | 79 | -169 | 73 | 57 | |
| JPC56 | 818 | 999-1001 | 12355 | 422 | 438 | -5 | 50 | 54 | -189 | 51 | 80 | -168 | 60 | 54 | |
| JPC56 | 818 | 1099-1101 | 13362 | 270 | 362 | 4 | 32 | 45 | -163 | 41 | 49 | -212 | 49 | 109 | BA |
| JPC56 | 818 | 1399-1401 | 14680 | 624 | 445 | 40 | 76 | 58 | -164 | 104 | 102 | -260 | 85 | 96 | |
| JPC56 | 818 | 1599-1601 | 15253 | 986 | 771 | 87 | 122 | 106 | -138 | 167 | 149 | -216 | 148 | 152 | H1 |
| JPC56 | 818 | 1699-1701 | 16688 | 493 | 495 | 208 | 70 | 75 | -143 | 76 | 102 | -131 | 80 | 91 | H1 |
| JPC56 | 818 | 1849-1851 | 17093 | 310 | 398 | 141 | 42 | 56 | -167 | 59 | 61 | -198 | 66 | 93 | H1 |
| JT96-09 | 920 | 47.5 | 10034 | 387 | 370 | -110 | 41 | 41 | -202 | 49 | 60 | -256 | 71 | 82 | |
| JT96-09 | 920 | 87.5 | 12365 | 422 | 454 | -12 | 49 | 56 | -195 | 50 | 81 | -171 | 61 | 54 | |
| JT96-09 | 920 | 112.5 | 13432 | 314 | 333 | -14 | 37 | 41 | -176 | 47 | 41 | -226 | 55 | 67 | BA |
| JT96-09 | 920 | 142.5 | 13619 | 347 | 307 | -32 | 40 | 37 | -195 | 42 | 43 | -261 | 128 | 94 | BA |
| JT96-09 | 920 | 261.5 | 14693 | 629 | 440 | -1 | 73 | 55 | -199 | 101 | 99 | -275 | 89 | 69 | |
| JT96-09 | 920 | 286.5 | 14880 | 761 | 560 | 14 | 89 | 71 | -204 | 103 | 127 | -262 | 109 | 81 | |
| JT96-09 | 920 | 346.5 | 16015 | 464 | 669 | 96 | 60 | 92 | -190 | 116 | 128 | -214 | 72 | 106 | H1 |
| KR02-15 PC6 | 2215 | 539.2 | 11134 | 537 | 472 | -119 | 55 | 52 | -237 | 61 | 78 | -266 | 64 | 57 | |
| KR02-15 PC6 | 2215 | 555.1 | 11535 | 439 | 506 | -147 | 44 | 54 | -264 | 69 | 71 | -288 | 80 | 70 | |
| KR02-15 PC6 | 2215 | 575.6 | 14788 | 720 | 423 | -16 | 82 | 52 | -221 | 99 | 107 | -282 | 98 | 62 | |
| KT89-18-P4 | 2700 | 185-190 | 10603 | 323 | 299 | -99 | 35 | 33 | -194 | 42 | 38 | -256 | 48 | 45 | |
| KT89-18-P4 | 2700 | 200-204 | 11841 | 453 | 344 | -64 | 49 | 40 | -205 | 69 | 62 | -217 | 58 | 42 | |
| KT89-18-P4 | 2700 | 236-240 | 12991 | 238 | 203 | -86 | 26 | 23 | -244 | 32 | 29 | -276 | 103 | 48 | |
| KT89-18-P4 | 2700 | 268-272 | 13816 | 319 | 211 | -110 | 40 | 16 | -257 | 43 | 21 | -352 | 48 | 28 | BA |
| KT89-18-P4 | 2700 | 338-342 | 15618 | 519 | 545 | 60 | 61 | 76 | -185 | 110 | 111 | -238 | 73 | 91 | H1 |
| KT89-18-P4 | 2700 | 449-453 | 20003 | 609 | 813 | 23 | 74 | 104 | -264 | 90 | 121 | -289 | 113 | 123 | LGM |
| KT89-18-P4 | 2700 | 534-538 | 22874 | 447 | 440 | 117 | 59 | 61 | -237 | 90 | 97 | -264 | 73 | 81 | LGM |

Table S4. cont.

Durations of BA, H1, and LGM are 13-14.5 ka, 15-17.5 ka, and 19-23 ka, respectively.

| Core ID | Water depth (m) | Core depth (cm) | Calendar age (yr) | -1 σ (yr) | +1 σ (yr) | Bottom $\Delta^{14}\text{C}$ (‰) | -1 σ (yr) | +1 σ (yr) | $\Delta^{14}\text{C}'$ cont-atm (‰) | -1 σ (yr) | +1 σ (yr) | $\Delta^{14}\text{C}'$ proj-atm (‰) | -1 σ (yr) | +1 σ (yr) | Era |
|-----------|--------------------|--------------------|----------------------|---------------------|---------------------|-------------------------------------|---------------------|---------------------|--|---------------------|---------------------|--|---------------------|---------------------|-----|
| MD97-2138 | 1900 | 207-210 | 21624 | 272 | 345 | 54 | 34 | 45 | -252 | 63 | 49 | -298 | 43 | 54 | LGM |
| MD97-2138 | 1900 | 211-215 | 21917 | 325 | 283 | 92 | 42 | 38 | -247 | 61 | 66 | -273 | 49 | 51 | LGM |
| MD98-2181 | 2100 | 1262-1268 | 19265 | 307 | 190 | 87 | 40 | 25 | -226 | 51 | 58 | -247 | 60 | 74 | LGM |
| MD98-2181 | 2100 | 1270-1276 | 19122 | 190 | 243 | 118 | 25 | 33 | -193 | 52 | 54 | -189 | 34 | 39 | LGM |
| MD98-2181 | 2100 | 1279-1285 | 19660 | 245 | 223 | 99 | 32 | 30 | -186 | 64 | 36 | -234 | 42 | 42 | LGM |
| MD01-2386 | 2800 | 198-203 | 10112 | 225 | 255 | -109 | 24 | 28 | -210 | 24 | 49 | -254 | 51 | 46 | |
| MD01-2386 | 2800 | 223-228 | 10938 | 211 | 221 | -108 | 22 | 24 | -215 | 43 | 40 | -266 | 25 | 33 | |
| MD01-2386 | 2800 | 248-253 | 12403 | 190 | 225 | -60 | 21 | 26 | -231 | 29 | 37 | -216 | 22 | 27 | |
| MD01-2386 | 2800 | 273-278 | 12974 | 206 | 165 | -36 | 24 | 19 | -201 | 31 | 25 | -222 | 64 | 61 | |
| MD01-2386 | 2800 | 298-303 | 13973 | 269 | 215 | -63 | 30 | 25 | -218 | 33 | 28 | -328 | 44 | 44 | BA |
| MD01-2386 | 2800 | 323-328 | 14180 | 367 | 341 | -51 | 41 | 40 | -207 | 60 | 49 | -314 | 59 | 57 | BA |
| MD01-2386 | 2800 | 348-353 | 15560 | 484 | 492 | 3 | 57 | 61 | -228 | 95 | 95 | -284 | 82 | 88 | H1 |
| MD01-2386 | 2800 | 373-378 | 16791 | 194 | 223 | 128 | 26 | 31 | -194 | 42 | 52 | -184 | 78 | 51 | H1 |
| MD01-2386 | 2800 | 398-403 | 16911 | 176 | 178 | 56 | 22 | 23 | -234 | 43 | 37 | -240 | 27 | 28 | H1 |
| MD01-2386 | 2800 | 423-428 | 17553 | 310 | 260 | 79 | 40 | 34 | -226 | 46 | 48 | -235 | 48 | 70 | |
| MD01-2386 | 2800 | 448-453 | 17672 | 254 | 299 | 35 | 31 | 38 | -256 | 39 | 39 | -243 | 54 | 52 | |
| MD01-2386 | 2800 | 473-478 | 18346 | 284 | 302 | 35 | 35 | 39 | -277 | 59 | 80 | -253 | 45 | 48 | |
| MD01-2386 | 2800 | 498-503 | 18978 | 250 | 282 | 77 | 32 | 37 | -209 | 62 | 42 | -214 | 92 | 55 | |
| MD01-2386 | 2800 | 523-528 | 19429 | 442 | 157 | 42 | 54 | 20 | -251 | 69 | 50 | -262 | 88 | 37 | LGM |
| MD01-2416 | 2317 | 88 | 13670 | 361 | 290 | -45 | 41 | 34 | -207 | 41 | 42 | -317 | 85 | 129 | BA |
| MD01-2416 | 2317 | 96 | 13530 | 318 | 293 | -104 | 34 | 32 | -250 | 42 | 34 | -360 | 48 | 49 | BA |
| MD01-2416 | 2317 | 115 | 14413 | 503 | 473 | -107 | 53 | 53 | -269 | 85 | 83 | -358 | 64 | 68 | BA |
| MD01-2416 | 2317 | 136 | 14242 | 494 | 565 | -183 | 47 | 58 | -316 | 85 | 72 | -408 | 83 | 71 | BA |
| MD01-2416 | 2317 | 163 | 15497 | 536 | 827 | -106 | 56 | 94 | -310 | 121 | 130 | -356 | 92 | 110 | H1 |
| MD01-2416 | 2317 | 177 | 17615 | 427 | 345 | -88 | 46 | 39 | -345 | 56 | 54 | -333 | 103 | 57 | |
| ODP1019 | 980 | 175 | 10277 | 457 | 373 | -97 | 49 | 42 | -184 | 64 | 45 | -255 | 66 | 83 | |
| ODP1019 | 980 | 251 | 10617 | 372 | 428 | -96 | 40 | 48 | -192 | 58 | 57 | -254 | 52 | 60 | |
| ODP1019 | 980 | 340 | 12467 | 415 | 467 | -136 | 42 | 50 | -293 | 47 | 69 | -317 | 129 | 101 | |
| ODP1019 | 980 | 380 | 12924 | 288 | 317 | -33 | 33 | 38 | -199 | 40 | 43 | -216 | 73 | 80 | |
| ODP1019 | 980 | 476 | 14614 | 589 | 471 | -7 | 68 | 58 | -198 | 101 | 98 | -280 | 86 | 74 | |
| ODP1019 | 980 | 580 | 17317 | 393 | 312 | 80 | 50 | 42 | -215 | 63 | 53 | -215 | 73 | 54 | H1 |
| ODP1019 | 980 | 713 | 18294 | 304 | 366 | 38 | 37 | 47 | -266 | 67 | 80 | -253 | 45 | 55 | |
| ODP1019 | 980 | 814 | 20992 | 499 | 433 | 179 | 69 | 63 | -177 | 93 | 106 | -189 | 80 | 88 | LGM |
| ODP883 | 2385 | 51 | 13698 | 373 | 292 | -13 | 44 | 35 | -181 | 43 | 44 | -240 | 136 | 88 | BA |
| ODP887 | 3647 | 52 | 12790 | 373 | 365 | -77 | 41 | 42 | -231 | 58 | 44 | -277 | 63 | 99 | |
| ODP887 | 3647 | 57.9 | 13503 | 306 | 292 | -54 | 34 | 34 | -206 | 46 | 33 | -308 | 95 | 122 | BA |
| ODP887 | 3647 | 63 | 14083 | 483 | 470 | -31 | 55 | 57 | -190 | 74 | 64 | -311 | 71 | 97 | BA |
| ODP887 | 3647 | 97 | 17244 | 351 | 308 | -15 | 41 | 37 | -278 | 58 | 42 | -282 | 61 | 54 | H1 |
| ODP887 | 3647 | 107 | 18952 | 281 | 313 | 16 | 34 | 39 | -254 | 62 | 44 | -293 | 44 | 50 | |
| ODP887 | 3647 | 112 | 18718 | 562 | 515 | -12 | 65 | 63 | -288 | 101 | 89 | -312 | 90 | 99 | |
| ODP887 | 3647 | 118 | 20298 | 686 | 577 | 18 | 81 | 74 | -267 | 95 | 94 | -286 | 129 | 85 | LGM |
| ODP893 | 588 | 1606 | 10550 | 353 | 459 | -73 | 39 | 53 | -174 | 50 | 64 | -244 | 49 | 106 | |
| ODP893 | 588 | 1652 | 10731 | 353 | 397 | -30 | 41 | 48 | -136 | 62 | 58 | -187 | 72 | 90 | |
| ODP893 | 588 | 1684 | 10707 | 343 | 405 | -28 | 40 | 49 | -135 | 59 | 60 | -187 | 68 | 94 | |
| ODP893 | 588 | 1696 | 10564 | 353 | 447 | -75 | 39 | 51 | -176 | 50 | 62 | -245 | 46 | 89 | |
| ODP893 | 588 | 1860 | 11942 | 530 | 586 | 40 | 65 | 76 | -131 | 88 | 107 | -133 | 83 | 78 | |
| ODP893 | 588 | 2005 | 12763 | 425 | 528 | 58 | 53 | 70 | -118 | 72 | 69 | -118 | 65 | 72 | |
| ODP893 | 588 | 2040 | 12947 | 325 | 344 | 72 | 41 | 46 | -111 | 48 | 50 | -103 | 51 | 46 | |
| ODP893 | 588 | 2194 | 13315 | 337 | 355 | 15 | 41 | 45 | -155 | 51 | 51 | -151 | 105 | 60 | BA |
| ODP893 | 588 | 2412 | 14317 | 520 | 528 | 42 | 64 | 69 | -135 | 101 | 87 | -241 | 116 | 156 | BA |
| ODP893 | 588 | 2558 | 16766 | 475 | 599 | 147 | 64 | 86 | -184 | 75 | 111 | -178 | 93 | 107 | H1 |
| ODP893 | 588 | 2680 | 17443 | 416 | 351 | 194 | 59 | 52 | -142 | 65 | 71 | -166 | 73 | 95 | H1 |
| ODP893 | 588 | 2873 | 18016 | 309 | 487 | 167 | 43 | 71 | -160 | 83 | 85 | -147 | 76 | 72 | |
| ODP893 | 588 | 3034 | 19101 | 297 | 314 | 185 | 42 | 46 | -141 | 68 | 62 | -147 | 56 | 69 | LGM |
| ODP893 | 588 | 3139 | 19703 | 301 | 424 | 226 | 44 | 65 | -104 | 70 | 74 | -116 | 55 | 70 | LGM |
| GC31 | 705 | 325.5 | 10790 | 200 | 200 | 56 | 25 | 26 | -59 | 39 | 30 | -85 | 24 | 66 | |
| GC31 | 705 | 349.5 | 11610 | 100 | 100 | -39 | 12 | 12 | -176 | 19 | 20 | -207 | 18 | 18 | |
| GC31 | 705 | 375.5 | 12410 | 200 | 200 | -164 | 20 | 20 | -315 | 29 | 32 | -362 | 103 | 83 | |
| GC31 | 705 | 411.5 | 13580 | 300 | 300 | -55 | 34 | 35 | -214 | 37 | 41 | -324 | 81 | 133 | BA |
| PC08 | 705 | 326 | 10810 | 200 | 200 | 6 | 24 | 25 | -103 | 41 | 30 | -126 | 58 | 39 | |
| PC08 | 705 | 341 | 11320 | 200 | 200 | 20 | 24 | 25 | -106 | 38 | 26 | -164 | 34 | 48 | |
| PC08 | 705 | 366 | 12120 | 200 | 200 | -181 | 20 | 20 | -315 | 31 | 26 | -366 | 92 | 68 | |
| PC08 | 705 | 391 | 12880 | 100 | 100 | -118 | 11 | 11 | -270 | 12 | 15 | -342 | 68 | 59 | |
| PC08 | 705 | 411 | 13570 | 100 | 100 | -29 | 12 | 12 | -191 | 16 | 19 | -251 | 51 | 49 | BA |
| PC08 | 705 | 422 | 13940 | 100 | 100 | -88 | 11 | 11 | -238 | 12 | 12 | -338 | 15 | 17 | BA |
| PC08 | 705 | 431 | 14200 | 200 | 200 | 55 | 25 | 26 | -118 | 36 | 30 | -164 | 103 | 44 | BA |
| PC08 | 705 | 437.5 | 14370 | 200 | 200 | -63 | 22 | 23 | -228 | 42 | 43 | -316 | 25 | 27 | BA |

Table S4. cont.

Durations of BA, H1, and LGM are 13-14.5 ka, 15-17.5 ka, and 19-23 ka, respectively.

| Core ID | Water depth (m) | Core depth (cm) | Calendar age (yr) | -1 σ (yr) | +1 σ (yr) | Bottom $\Delta^{14}\text{C}$ (‰) | -1 σ (yr) | +1 σ (yr) | $\Delta^{14}\text{C}'$ cont-atm (‰) | -1 σ (yr) | +1 σ (yr) | $\Delta^{14}\text{C}'$ proj-atm (‰) | -1 σ (yr) | +1 σ (yr) | Era |
|-------------|--------------------|--------------------|----------------------|---------------------|---------------------|-------------------------------------|---------------------|---------------------|--|---------------------|---------------------|--|---------------------|---------------------|-----|
| PC08 | 705 | 447.5 | 14650 | 100 | 100 | -172 | 10 | 10 | -333 | 20 | 18 | -411 | 17 | 20 | |
| PC08 | 705 | 456.5 | 14960 | 200 | 200 | -151 | 20 | 21 | -334 | 24 | 29 | -392 | 28 | 32 | |
| PC08 | 705 | 466 | 15300 | 300 | 300 | -184 | 29 | 30 | -356 | 51 | 38 | -419 | 45 | 61 | H1 |
| PC08 | 705 | 476.5 | 15670 | 300 | 300 | -176 | 29 | 30 | -369 | 58 | 53 | -402 | 46 | 52 | H1 |
| PC08 | 705 | 486.5 | 16020 | 300 | 300 | -128 | 31 | 32 | -355 | 62 | 62 | -373 | 52 | 58 | H1 |
| PC08 | 705 | 496.5 | 16370 | 300 | 300 | -62 | 33 | 35 | -329 | 50 | 56 | -332 | 47 | 65 | H1 |
| PC08 | 705 | 506.5 | 16730 | 300 | 300 | -16 | 35 | 36 | -301 | 46 | 59 | -279 | 69 | 46 | H1 |
| PC08 | 705 | 516.5 | 17080 | 300 | 300 | 22 | 36 | 38 | -254 | 52 | 46 | -273 | 49 | 68 | H1 |
| PC08 | 705 | 526.5 | 17430 | 300 | 300 | 98 | 39 | 41 | -210 | 48 | 57 | -202 | 63 | 53 | H1 |
| PC08 | 705 | 536.5 | 17780 | 300 | 300 | 139 | 41 | 42 | -185 | 44 | 50 | -172 | 66 | 54 | |
| PC08 | 705 | 547 | 18120 | 300 | 300 | 105 | 39 | 41 | -199 | 79 | 54 | -192 | 63 | 57 | |
| PC08 | 705 | 556 | 18410 | 300 | 300 | 163 | 41 | 43 | -197 | 52 | 93 | -164 | 60 | 68 | |
| PC08 | 705 | 641.5 | 21140 | 200 | 200 | 108 | 26 | 27 | -232 | 30 | 35 | -243 | 66 | 63 | LGM |
| PC08 | 705 | 661.5 | 21770 | 300 | 300 | 208 | 43 | 45 | -155 | 69 | 65 | -177 | 76 | 84 | LGM |
| PC08 | 705 | 680.8 | 22390 | 300 | 300 | 300 | 46 | 48 | -100 | 62 | 64 | -114 | 78 | 87 | LGM |
| PC4/PC5 | 1366 | 231-232 | 11115 | 527 | 462 | -68 | 58 | 54 | -193 | 62 | 80 | -210 | 87 | 43 | |
| PC4/PC5 | 1366 | 262-264 | 11589 | 454 | 469 | -80 | 49 | 54 | -213 | 69 | 78 | -233 | 59 | 58 | |
| PC4/PC5 | 1366 | 291-293 | 12263 | 406 | 442 | -81 | 44 | 50 | -239 | 60 | 65 | -232 | 94 | 69 | |
| PC4/PC5 | 1366 | 311-313 | 13191 | 345 | 279 | -98 | 37 | 31 | -253 | 43 | 39 | -356 | 77 | 109 | BA |
| PC4/PC5 | 1366 | 363-365 | 14756 | 694 | 430 | 11 | 81 | 54 | -196 | 101 | 106 | -267 | 95 | 71 | |
| PC4/PC5 | 1366 | 405-407 | 16029 | 461 | 662 | 97 | 60 | 92 | -189 | 115 | 126 | -212 | 72 | 105 | H1 |
| PC4/PC5 | 1366 | 540-542 | 18763 | 250 | 499 | 75 | 32 | 67 | -226 | 57 | 83 | -220 | 51 | 68 | |
| PC4/PC5 | 1366 | 642-644 | 20638 | 393 | 462 | 52 | 49 | 60 | -233 | 96 | 74 | -283 | 81 | 95 | LGM |
| TR163-31 | 3210 | 83-87 | 17291 | 429 | 381 | 153 | 58 | 54 | -159 | 74 | 62 | -186 | 80 | 90 | H1 |
| TR163-31 | 3210 | 114 | 19269 | 446 | 492 | -93 | 48 | 56 | -355 | 59 | 90 | -365 | 94 | 74 | LGM |
| VM21-30 | 617 | 139 | 10848 | 369 | 351 | -450 | 24 | 24 | -513 | 45 | 40 | -602 | 63 | 49 | |
| VM21-30 | 617 | 143 | 10587 | 369 | 461 | -541 | 20 | 26 | -590 | 37 | 39 | -673 | 39 | 53 | |
| VM21-30 | 617 | 177 | 13233 | 334 | 335 | -590 | 16 | 17 | -661 | 24 | 27 | -724 | 29 | 28 | BA |
| VM21-30 | 617 | 182 | 13594 | 486 | 423 | -492 | 29 | 27 | -577 | 34 | 33 | -639 | 61 | 44 | BA |
| VM21-30 | 617 | 201-202 | 16506 | 864 | 683 | -413 | 58 | 51 | -582 | 85 | 98 | -607 | 70 | 65 | H1 |
| VM21-30 | 617 | 236 | 20087 | 506 | 303 | 51 | 62 | 39 | -247 | 69 | 66 | -276 | 72 | 62 | LGM |
| VM21-30 | 617 | 241 | 19546 | 586 | 417 | -268 | 50 | 38 | -467 | 74 | 58 | -514 | 80 | 61 | LGM |
| W8709A-13PC | 2712 | 126.25 | 10291 | 553 | 432 | -178 | 53 | 44 | -257 | 67 | 12 | -324 | 54 | 57 | |
| W8709A-13PC | 2712 | 139 | 11313 | 549 | 430 | -138 | 55 | 46 | -244 | 76 | 59 | -284 | 56 | 53 | |
| W8709A-13PC | 2712 | 154 | 11979 | 543 | 436 | -116 | 56 | 48 | -259 | 76 | 78 | -261 | 111 | 69 | |
| W8709A-13PC | 2712 | 170.5 | 13151 | 343 | 272 | -37 | 39 | 32 | -202 | 45 | 39 | -246 | 59 | 86 | BA |
| W8709A-13PC | 2712 | 191.5 | 13752 | 409 | 294 | -113 | 43 | 32 | -263 | 43 | 40 | -355 | 52 | 43 | BA |
| W8709A-13PC | 2712 | 198.75 | 14099 | 508 | 477 | -117 | 53 | 52 | -263 | 71 | 61 | -365 | 64 | 69 | BA |
| W8709A-13PC | 2712 | 212.5 | 15289 | 730 | 760 | 0 | 85 | 96 | -208 | 133 | 120 | -282 | 108 | 116 | H1 |
| W8709A-13PC | 2712 | 221.25 | 15889 | 633 | 650 | -61 | 69 | 77 | -298 | 126 | 132 | -324 | 102 | 98 | H1 |
| W8709A-13PC | 2712 | 223.75 | 15849 | 607 | 621 | -45 | 68 | 75 | -284 | 123 | 128 | -319 | 97 | 103 | H1 |
| W8709A-13PC | 2712 | 301.25 | 19018 | 291 | 304 | 15 | 35 | 38 | -256 | 65 | 45 | -291 | 50 | 52 | LGM |
| W8709A-13PC | 2712 | 303.75 | 19261 | 376 | 282 | 11 | 45 | 35 | -281 | 55 | 69 | -282 | 84 | 46 | LGM |

Table S5. Averaged ventilation proxies during LGM, H1, and BA in the eastern and western North Pacific (water depths ranging 900 to 2800 m)

| Area | Era | BF-PF (yr) | $\pm 1\sigma$ (yr) | Projection (yr) | $\pm 1\sigma$ (yr) | $\Delta^{14}\text{C}'$ cont-atm (‰) | $\pm 1\sigma$ (‰) | $\Delta^{14}\text{C}'$ proj-atm (‰) | $\pm 1\sigma$ (‰) | |
|------------|-----|---------------|-----------------------|--------------------|-----------------------|--|----------------------|--|----------------------|-----|
| NW Pacific | LGM | 1283 | 303 | 1767 | 335 | -235 | 37 | -267 | 35 | n=5 |
| NW Pacific | H1 | 870 | 250 | 1105 | 385 | -198 | 35 | -209 | 34 | n=5 |
| NW Pacific | BA | 1181 | 442 | 2573 | 717 | -238 | 37 | -335 | 40 | n=7 |
| NE Pacific | LGM | 1347 | 585 | 1721 | 638 | -255 | 43 | -274 | 52 | n=3 |
| NE Pacific | H1 | 1317 | 316 | 1585 | 532 | -235 | 40 | -260 | 51 | n=6 |
| NE Pacific | BA | 1074 | 387 | 2111 | 898 | -217 | 39 | -303 | 72 | n=5 |

References

- S1 H. Goosse, E. Deleersnijder, T. Fichefet, M. H. England, *J. Geophys. Res.-Oceans* **104**, 13681 (1999).
- S2 A. L. Berger, *Journal of the Atmospheric Sciences* **35**, 2362 (1978).
- S3 V. Brovkin, A. Ganopolski, Y. Svirezhev, *Ecol. Model.* **101**, 251 (1997).
- S4 A. Mouchet, L. M. Francois, *Phys. Chem. Earth* **21**, 511 (1996).
- S5 L. Menviel, A. Timmermann, A. Mouchet, O. Timm, *Paleoceanography* **23**, (2008).
- S6 J. R. Southon, D. E. Nelson, J. S. Vogel, *Paleoceanography* **5**, 197 (1990).
- S7 D. J. Kovanen, D. J. Easterbrook, *Geology* **30**, 243 (2002).
- S8 Y. V. Kuzmin, G. S. Burr, A. J. T. Jull, *Radiocarbon* **43**, 477 (2001).
- S9 Y. V. Kuzmin, G. S. Burr, S. V. Gorbunov, V. A. Rakov, N. G. Razjigaeva, *Nucl. Instrum. Methods Phys. Res. Sect. B-Beam Interact. Mater. Atoms* **259**, 460 (2007).
- S10 M. Yoneda *et al.*, *Nucl. Instrum. Methods Phys. Res. Sect. B-Beam Interact. Mater. Atoms* **259**, 432 (2007).
- S11 E. D. Galbraith *et al.*, *Nature* **449**, 890 (2007).
- S12 M. Shishikura, T. Echigo, H. Kaneda, *Quat. Res.* **67**, 286 (2007).
- S13 M. Butzin, M. Prange, G. Lohmann, *Earth Planet. Sci. Lett.* **235**, 45 (2005).
- S14 W. Broecker *et al.*, *Science* **306**, 1169 (2004).
- S15 L. C. Skinner, N. J. Shackleton, *Quat. Sci. Rev.* **24**, 571 (2005).
- S16 M. Okada, M. Takagi, H. Narita, K. Takahashi, *Deep-Sea Res. Part II-Top. Stud. Oceanogr.* **52**, 2092 (2005).
- S17 J. F. Adkins, E. A. Boyle, *Paleoceanography* **12**, 337 (1997).
- S18 P. J. Reimer *et al.*, *Radiocarbon* **51**, 1111 (2009).
- S19 N. J. Shackleton *et al.*, *Nature* **335**, 708 (1988).
- S20 M. Sarnthein, T. Kiefer, P. M. Grootes, H. Elderfield, H. Erlenkeuser, *Geology* **34**, 141 (2006).
- S21 L. Stott, J. Southon, A. Timmermann, A. Koutavas, *Paleoceanography* **24**, (2009).
- S22 T. M. Marchitto, S. J. Lehman, J. D. Ortiz, J. Fluckiger, A. van Geen, *Science* **316**, 1456 (2007).
- S23 P. R. Bevington, D. K. Robinson, *Data reduction and error analysis for the physical sciences* (McGraw-Hill, 1969).
- S24 K. Ohkushi, N. Ahagon, M. Uchida, Y. Shibata, *Geochem. Geophys. Geosyst.* **6**,

- (2005).
- S25 A. vanGeen *et al.*, *Paleoceanography* **11**, 519 (1996).
- S26 L. D. Keigwin, *J. Oceanogr.* **58**, 421 (2002).
- S27 J. L. McKay, T. F. Pedersen, J. Southon, *Paleoceanography* **20**, (2005).
- S28 A. C. Mix *et al.*, in *Mechanisms of Global Climate Change at Millennial Time Scales* P. U. Clark, R. S. Webb, L. D. Keigwin, Eds. (American Geophysical Union, Washington DC, 1999), pp. 127-148.
- S29 J. P. Kennett, B. L. Ingram, *Nature* **377**, 510 (1995).
- S30 A. deVernal, T. F. Pedersen, *Paleoceanography* **12**, 821 (1997).
- S31 R. Zahn, T. F. Pedersen, B. D. Bornhold, A. C. Mix, *Paleoceanography* **6**, 543 (1991).
- S32 J. C. Duplessy *et al.*, *Radiocarbon* **31**, 493 (1989).
- S33 K. Ikehara, K. Ohkushi, A. Shibahara, M. Hoshiba, *Glob. Planet. Change* **53**, 78 (2006).
- S34 T. Sagawa, K. Ikehara, *Geophys. Res. Lett.* **35**, (2008).
- S35 K. Minoshima *et al.*, *Nucl. Instrum. Methods Phys. Res. Sect. B-Beam Interact. Mater. Atoms* **259**, 448 (2007).
- S36 M. Murayama, A. Taira, H. Iwakura, E. Matsumoto, T. Nakamura, *Summaries of Researches using AMS at Nagoya University* **3**, 114 (1992).
- S37 N. Ahagon, K. Ohkushi, M. Uchida, T. Mishima, *Geophys. Res. Lett.* **30**, (2003).
- S38 M. Hoshiba *et al.*, *Mar. Micropaleontol.* **61**, 196 (2006).
- S39 Y. Okazaki *et al.*, *Deep-Sea Res. Part II-Top. Stud. Oceanogr.* **52**, 2150 (2005).
- S40 W. S. Broecker, T. H. Peng, S. Trumbore, G. Bonani, W. Wolfli, *Global Biogeochemical Cycles* **4**, 103 (1990).
- S41 W. Broecker, E. Clark, S. Barker, *Earth Planet. Sci. Lett.* **274**, 322 (2008).